# Comparison of the degradations of diphenamid by homogeneous photolysis and heterogeneous photocatalysis in aqueous solution

Hai-chao Liang[a], Xiang-zhong Li[a,*], Yin-hua Yang[b], Kong-hung Sze[b,**]

[a] *Department of Civil and Structural Engineering, The Hong Kong Polytechnic University, Hong Kong, China*

[b] *Department of Chemistry, The University of Hong Kong, Hong Kong, China*

*Corresponding author. Tel.: +852 2766 6016; Fax: +852 2334 6389; E-mail address: cexzli@polyu.edu.hk*

*Second Corresponding author: Tel.: +852 2859 7915; Fax: +852 2857 1586; E-mail address: khsze@hkucc.hku.hk*

Abstract

In this work, the homogeneous and heterogeneous degradations of diphenamid (DPA) in aqueous solution were conducted by direct photolysis with UVC (254 nm) and by photocatalytsis with $TiO_2$/UVA (350 nm), and the experimental results were compared. It was found that the homogeneous photolysis by UVC irradiation alone was quite efficient to degrade DPA up to 100% after 360 min, but was very inefficient to mineralize its intermediates in terms of dissolved organic carbon reduction of only 8%. In contrast, the heterogeneous photocatalysis with $TiO_2$/UVA showed relatively a lower degree of DPA degradation (51%), but a higher degree of its mineralization (11%) after 360 min. These results reveal that the photocatalysis process has relatively poor selectivity to degrade different compounds including various intermediates from the DPA degradation, which is beneficial to its mineralization. In addition, over 20 intermediates were identified by LC-MS and ^{1}H-NMR analyses. Based on the identified intermediates, the reaction mechanisms and the detailed pathways of the DPA degradation by photolysis and photocatalysis were proposed, and are presented in this paper.

31
32
33    **1. Introduction**

34

35    Diphenamid (DPA) as a pre-emergent herbicide is widely employed for control of annual

36    grasses and broadleaf weeds in tomato, potato, peanut, and soybean plants (Schultz and

37    Tweedy, 1972; Sirons et al., 1981). This substance does enter the environment under normal

38    use or through inappropriate disposal and is harmful to aquatic organisms. Therefore, the

39    investigation of remediation treatments of polluted waters containing trace amounts of

40    herbicides is of environmental interests.

41    In the past decades, research on the photochemical degradation of DPA in aqueous

42    solution has progressed quickly because of the high efficiency of mineralization under the

43    mild operating conditions (Rosen, 1967; Schultz and Tweedy, 1972; Rahman et al., 2003).

44    For example, Rosen (1967) studied the homogeneous photodegradation of DPA by UV and

45    sunlight irradiation, but the mechanism and the major products from DPA degradation were

46    not well identified. Rahman et al. (2003) investigated the photocatalytic degradation of DPA

47    in aqueous P25 $TiO_2$ suspension under the illumination of a medium pressure mercury lamp.

48    Although they identified five intermediates using a GC-MS technique and suggested a brief

49    pathway of the DPA degradation, the five products identified in their study were not

50    sufficient enough to buildup a thorough pathway delineating the photocatalytic degradation

51    of DPA due to the complexity of the DPA molecular structure. Furthermore, the medium

52    pressure mercury lamp used in their experiment offers a broad band of light emission from

53    200 to 600 nm, thus resulting in both types of processes, homogeneous photolysis and

54    heterogeneous photocatalysis, to possibly occur in the DPA degradation. In short, the

55    literatures reported previously did not supply a clear clarification of the photochemical

56    reactions for the degradation of DPA pollutants in water. Therefore, in order to better

57    understand the difference of DPA degradation by homogeneous photolysis and heterogeneous

58    photocatalysis, two sets of experiments for DPA degradation in aqueous solution by direct

59    photolysis with UVC and photocatalysis with $TiO_2$/UVA were conducted in this study. In

60    which, the reaction mechanisms and pathways of DPA degradation by direct photolysis and

61    photocatalysis were proposed based on over 20 intermediates identified by the combination

62    of ^{1}H-NMR and LC-MS analyses.

63

64    **2. Experimental**

65    *2.1. Materials*

66       DPA chemical (99.9%) was purchased from Aldrich Chemical Company. Self-prepared

67    $TiO_2$ films as reported before (Liang and Li, 2009) were used as photocatalysts. 0.5 M HCl and

68    0.5 M NaOH solutions were used to adjust the solution pH. Other chemicals such as $CDCl_3$ and

69    $CH_3CN$ (Aldrich) were used without further purification. Deionized distilled water was used

70    throughout the experiments.

71

72    *2.2. Experimental setup and procedure*

73       A UV–photoreactor system consists of a quartz reactor, an external UV light source, one

74    piece of $TiO_2$ film with an area of 3 $cm^2$, and 25 mL of aqueous DPA solution. The UV lamp

75    was placed perpendicularly on the top of the reactor and the distance between the lamp and

76    the surface of solutions was ~6 cm (see Supplemental Material (SM), Fig. SM-1). In order to

77    compare the effect of UV wavelengths on the photochemical behavior of direct photolysis

78    and photocatalysis, DPA solutions were irradiated with different UV lamps: (a) UVC region,

79    using a G8T5 germicidal lamp with a maximum at 254 nm (Sankyo Denki Co. Ltd., Japan);

80    (b) UVA region, using a F8T5/BL-B black light blue lamp with a wavelength range of 318-

81   400 nm and its main emission at 350 nm (Hitachi, Japan). Both UV lamps had an equivalent

82   power consumption of 8 W and the corresponding light intensity detected in the experiment

83   was $8.02 \times 10^{-4}$ W cm$^{-2}$ for UVC and $1.01 \times 10^{-3}$ W cm$^{-2}$ for UVA, respectively. Prior to

84   photocatalytic reaction, the DPA solution of 20 mg L$^{-1}$ was magnetically stirred in the dark

85   for 60 min in order to achieve adsorption/desorption equilibrium. Then the DPA

86   concentration (~19.2 mg L$^{-1}$) in the bulk solution at this time was used as an initial value. All

87   reactions were performed at room temperature of ~21 $^{o}$C. During the photocatalytic reaction,

88   the samples were collected from the solution at different intervals.

89

90   *2.3. Chemical analysis*

91   The DPA concentration was determined by HPLC (Finnigan SpectraSYSTEM P4000)

92   consisting of a Pinnacle II C18 reverse-phase column (5 μm, 4.6 mm × 250 mm) and a UV

93   detector (UV 6000LP) at 254 nm. The mobile phase consisted of acetonitrile/water (v:v = 3:2)

94   with 0.5 vol% acetic acid/phosphoric acid, and flowed at 1.0 mL min$^{-1}$. In order to identify

95   the organic reaction intermediate species, combination of LC-MS and $^{1}$H-NMR analyses

96   were employed. All one-dimensional and two-dimensional (2D) $^{1}$H-NMR spectra were

97   recorded at ambient temperature using a NMR spectrometer (Bruker Avance 600 MHz)

98   equipped with a tick carboxypeptidase inhibitor cryoprobe. To avoid missing out any

99   intermediates at a low concentration during the NMR analysis, it is necessary to extract the

100  organic substrates in the final water samples with chloroform (HPLC grade) before the NMR

101  detection. Although the DPA solutions with an initial concentration of 20 mg L$^{-1}$ were used in

102  the experiments to determine the kinetic reaction rate constants (k) of photolysis and

103  photocatalysis reactions, the higher concentration of DPA at 130 mg L$^{-1}$ was used in the

104  experiments to identify the intermediates by $^{1}$H-NMR analysis. In the meantime, an ion trap

105  mass spectrometer (Finnigan LCQ$^{TM}$ DUO) coupled to LC-MS was also used to further verify

106    the reaction intermediates through electrospray ionization (ESI). The ESI probe was installed

107    with sheath and auxiliary gasses at 60 and 20 units, respectively. The mass spectrometer was

108    operated in the positive/negative ion mode in the m/z 50-400 range for LC-MS and LC-

109    MS/MS. The MS conditions were set at capillary temperature = 250 $^{o}$C, voltage = 46 V and

110    spray voltage = 4.5 kV.

111        Dissolved organic carbon (DOC) concentration was determined by a total organic carbon

112    (TOC) analyzer (TOC-5000A, Shimadzu, Japan) equipped with an auto-sampler (ASI-5000).

113    $O_2$ as a carrier gas was used in the detecting system. In this analysis, organic carbon = total

114    carbon (TC) – inorganic carbon (IC). Under the acidic condition, all inorganic carbon was

115    converted to $CO_2$ and measured. Prior to the TOC analysis, two standard solutions, potassium

116    hydrogen phthalate (KOOC•$C_6H_4$•COOH) solutions in the range of 10-100 mg L$^{-1}$ and

117    sodium carbonate ($Na_2CO_3$) solutions of 1-10 mg L$^{-1}$, were used to calibrate TC and IC

118    concentrations respectively. The minimum acceptable correlation coefficient ($R^2$) was 0.9991

119    and the detection limit of the method was 0.1 mg L$^{-1}$.

120

121    **3. Results and discussion**

122

123    *3.1. Direct photolysis and photocatalysis of DPA in aqueous solutions*

124        The photodecay of DPA by UV light radiation with and without catalyst is thought to

125    follow the pseudo-first-order reaction with respect to the DPA concentration (Rahman et al.,

126    2003). In this study, the semi-log graphs of the DPA degradation by photolysis and

127    photocatalysis versus irradiation time yield straight lines, indicating the pseudo-first-order

128    reaction kinetics. The reaction rate constants ($k$) were evaluated from the experimental data

129    by the linear regression. In all cases $R^2$ values are higher than 0.97, indicating that the

130    exponential model can well describe the kinetics for DPA degradation in both processes.

131  DOC was also monitored to compare the degree of DPA mineralization in both processes at

132  different pH.

133

134  [Table 1]

135

136      The two sets of experiments in aqueous DPA solutions without TiO$_2$ film at pH 3.5, 7.2

137  and 9.6 were first conducted under UVC and UVA illumination, respectively for 360 min.

138  The experimental results are shown in Table 1. It can be seen that while the direct photolysis

139  with UVA showed almost no reduction of DPA after 360 min at three pH values, the direct

140  photolysis with UVC showed that, DPA was degraded by 100% after 360 min at pH 3.5, 7.2

141  and 9.6, but the corresponding DOC was only reduced by 11, 8 and 9%, respectively. These

142  results indicate that DPA cannot be degraded by direct photolysis under UVA illumination

143  (350 nm) because of its main light absorption at ~260 nm, but it can be excited by UVC light

144  (254 nm) and then quickly degraded through direct electron transfer reaction. However, the

145  direct UVC-photolysis had poor mineralization when the DOC removal is considered to

146  reflect the degree of mineralization. The effect of pH on DPA degradation indicated that DPA

147  was degraded from fast to slow in an order of pH 3.5 > 9.6 > 7.2. It can be attributed to the

148  unique ionic states of DPA under acidic and alkaline conditions. Both the acidic and alkaline

149  conditions favored UV absorption by DPA (Fig. SM-2), resulting in faster homolytic or

150  heterolytic breakages in the DPA molecules. With the further photolysis reaction, some acidic

151  products were formed from the DPA degradation.

152

153      To conduct a photocatalysis reaction without direct photolysis, aqueous DPA solution in

154  presence of TiO$_2$ film was irradiated by the UVA light in the wavelength range of 318-400

155  nm under different pH conditions and the experimental results are also presented in Table 1.

156   It can be seen that at pH 3.5, DPA was degraded by 63% and DOC was reduced by 13% after

157   360 min whereas at pH 9.6, DPA was degraded by 42% and DOC by 8%. These results

158   indicate that DPA can be degraded by the photocatalysis with $TiO_2$/UVA, but more slowly

159   than that by the photolysis with UVC. Furthermore, it was found that under acidic and neutral

160   conditions, the DOC removal by the photocatalysis (13 and 11%, respectively) was higher

161   than that by photolysis (11 and 8%, respectively). These results might indicate that

162   photocatalysis process has poor selectivity for degrading different intermediates from the

163   DPA degradation, which is beneficial to DPA mineralization, especially under the acidic

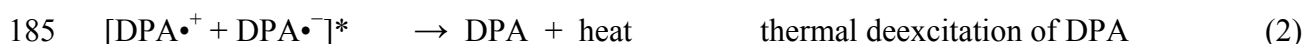164   condition, while the direct photolysis showed the relatively lower DOC removals.

165

166   *3.2. Mechanism of homogeneous and heterogeneous DPA degradation*

167   $TiO_2$-based photocatalysis is well known to produce •OH radicals in water, through the

168   interface oxidation of hydroxide anions or water molecules adsorbed on the semiconductor

169   surface by the holes photogenerated in the valence band of semiconductor. The •OH radicals

170   produced by $TiO_2$ are the powerful oxidizing species and can initiate the degradation of

171   aromatic compounds by direct attack to the aromatic rings, leading to the formation of

172   hydroxylated intermediate species (as shown in the later discussion). At sufficient contact

173   time and proper operation conditions, it is practically possible to mineralize the target

174   pollutant to $CO_2$ and $H_2O$. This property results in good mineralization for the $TiO_2$/UVA

175   photocatalysis. However, it should be noted that the photocatalytic process mainly occurs on

176   the photocatalyst surface, but not in the bulk solution; in other words, the photocatalytic

177   process depends on the adsorption and diffusion of DPA/intermediate molecules on the $TiO_2$

178   surface, thus leading to a slow rate of DPA degradation.

179   In contrast, the mechanism of the direct UVC-induced photolysis ($\lambda$ = 254 nm) is based

180   on the fact that the chemical species undergo the homogeneous reactions in solution, by

181  which molecules are broken down to smaller molecules as a result of photodecomposition of

182  the excited organic compounds. The sequence of events that could occur during a particular

183  DPA photolytic decomposition is summarized below.

184  $DPA + h\nu \rightarrow DPA^* \rightarrow [DPA\bullet^+ + DPA\bullet^-]^*$    excitation of DPA            (1)

185  $[DPA\bullet^+ + DPA\bullet^-]^* \rightarrow DPA + heat$        thermal deexcitation of DPA       (2)

186  $[DPA\bullet^+ + DPA\bullet^-]^* \rightarrow I_{uv}$    decomposition of DPA and formation of intermediates  (3)

187  $I_{uv} + h\nu \rightarrow I_{uv}^*$          excitation of intermediates         (4)

188  $I_{uv}^* \rightarrow$ products        decomposition of intermediates      (5)
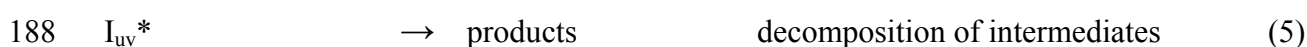
189
190  Here Eq. 1 involves the excitation of DPA, in which the photo-excited state of $DPA^*$ takes

191  one-electron from the ground state of DPA molecule to produce radical anion $DPA\bullet^-$.

192  Subsequent reaction can either undergo thermal deexcitation (Eq. 2) via recombination of

193  radical ions or photodecomposition to produce intermediate $I_{uv}$ (Eq. 3). Some intermediates

194  $I_{uv}$ can also absorb UV light to produce excited state intermediate $I_{uv}^*$ as shown in Eq. 4,

195  further undergoing the decomposition towards final products step by step (Eq. 5), but some

196  cannot when energy absorbed by intermediate molecules directly from UV light is not

197  enough to cause the bond scission. The formation of resistant intermediates just explains the

198  fact that generally direct photolysis has a lower degree of mineralization than that of

199  photocatalysis with $TiO_2$.

200
201
202  *3.3. Identification of intermediates*

203     Both the LC-MS and $^1$H-NMR analyses were used to detect the intermediates. It should

204  be noted that the NMR technique can avoid the escaping of some polar intermediates and

205  positional isomers generally occurring in the MS analysis alone. Table 2 and Table SM-1

206  summarized the analytical results along with the proposed structures for the detected

207     byproducts, in which 21 intermediate products were identified according to the mass ion

208     peaks from MS spectra and the characteristic proton patterns from ^{1}H-NMR spectra. Three

209     principal groups of intermediate products were identified in both homogeneous and

210     heterogeneous degradation processes: (i) products 1–4 from the reactions relevant to only the

211     *N*-methyl oxidation or replacement; (ii) products 5–12 from the reactions of the

212     hydroxylation of the aromatic ring; and (iii) products 13–21 from the N-demethylation,

213     oxidation and ring opening. The intermediate products 1-7 were listed in Table 2 and other

214     products 8-21 were shown in Table SM-1.

215

216     [Table 2]

217

218         In this paper, both positive and negative ion full-scan mode experiments over the mass

219     range from $m/z$ 50 to 400 were used to determine the $m/z$ of the individual components

220     related to DPA and its degradation products, as shown in Fig. 1. For comparison, the

221     fragmentation pattern obtained from photolysis (Fig. 1a) was analogous to that of $TiO_2$-

222     photocatalysis (Fig. 1b), for the most part, and supports the assigned structure (see Table 2).

223     For example, the major ions with $m/z$ 256 and 272, corresponding to mono- and bi-

224     hydroxylation respectively, were both observed in spectra (a) and (b). The major ion with $m/z$

225     333 is due to the couple of fragments of $-CH(C_6H_5)_2$, whereas the minor ion ($m/z$ 196) should

226     be interpreted as arising from cleavage of the bond between the carbonyl group and the N-

227     dimethyl group. By analogy, formation of fragment ions at $m/z$ 105 and 123 in MS spectra of

228     byproducts 18 and 19 can be rationalized. The structures of the identified fragments ($m/z$ 287,

229     301, 316, 366) are shown in Table SM-1. It should be pointed out that this type of

230     fragmentation was already observed for iodosulfuron degradation by Sleiman et al. (2006).

231         [Fig. 1]

9

232

233    Some of ^{1}H-NMR spectra were used to further determine the chemical structures of the

234    degradation products of DPA as shown in Fig. 2. Figure 2a depicts the *p*-, *o*- and *m*- regions

235    (5.35–5.70 ppm) of the 2D-COSY spectra of DPA solutions after the irradiation by direct

236    UVC photolysis for 1 h and by $TiO_2$/UVA photocatalysis for 24 h. This is the time at which

237    the DPA degradation exceeded 50% and the concentrations of its products were sufficient to

238    be observed clearly in the NMR analysis. 2D-COSY analysis was conducted in our study

239    because in a COSY spectrum the coupling interaction is generally allowed to identify which

240    protons couple to each other. From Fig. 2a, it is interesting to find that for the DPA molecule

241    there is the existence of a strong cross peak that corresponds to the chemical shifts of both

242    protons, in which the horizontal line from the spot at 3.00 ppm corresponds to the methyl

243    protons while the vertical line drawn from the spot at 5.58 ppm corresponds to the methine

244    protons. The presence of this cross peak, which correlates the methyl protons and methine

245    protons, confirms that (1) such COSY method can detect the long-range coupling interaction

246    that extends to five bonds (Pavia et al., 2001) and (2) the methyl and methine groups must be

247    present simultaneously in DPA molecules. Besides this, other four types of cross peaks,

248    similar to the nature of DPA molecule, were also observed in this COSY spectrum. They are

249    nonequivalent, probably owing to the nuclear magnetization effect of the methyl neighbor

250    group. Therefore, combining the specific proton information with corresponding MS data,

251    the four intermediates can be identified as compounds 1–4 arising from oxidation or removal

252    of terminal N-methyl group in DPA molecule, simultaneously appearing in the UVC

253    photolysis and $TiO_2$/UVA photocatalysis processes.

254

255    [Fig. 2]

256

257    The second category of products includes different phenolic compounds resulting from

258    the hydroxylation of benzene ring during the UVC and TiO$_2$/UVA processes. The different

259    intermediates reflect the difference in the reaction mechanisms of two processes: the

260    homogeneous degradation of DPA by photolysis is dependent upon the bond strength of

261    DPA/intermediate molecules and their energy absorbing ability, while the heterogeneous

262    degradation of DPA by photocatalysis is mainly affected by the attack of •OH radicals.

263    Among these products, compounds 5, 6 and 7 are positional isomers and they were

264    discriminated by ^{1}H-NMR rather than MS analysis. Since the chemical shift of ortho-proton

265    of most phenolic compounds is 6.0–7.0 ppm in many literatures (Limiroli et al., 1996; Es-Safi

266    et al., 2000), the evolution of main products belonging to this group is represented on the

267    NMR spectra in the region of 6.0–7.2 ppm, as shown in Fig. 2b. It can be clearly observed

268    that some strong proton signals occurred in the spectrum (C). According to the mass of 256

269    m/z, compounds 5, 6 and 7 would be recognized with the monosubstitution by OH in the

270    para-, ortho- and meta-position, respectively. While compounds 6 and 7 had the same

271    concentration level, compound 5 showed the higher concentration level of about 4.5 times

272    than that of compounds 6 and 7. This result indicates that compound 5 is a major

273    hydroxylated product from the DPA degradation by TiO$_2$/UVA due to the regioslective attack

274    of •OH. This can be explained by the electron density of the benzene carbon sites and the

275    steric hindering effects of the benzene ring substituents (–CHCON(CH$_3$)$_2$), where the para-

276    position is more nucleophilic and accessible than the other two positions at ortho and meta

277    orientation. In contrast, spectrum (B) in Fig. 2b shows very low proton signals of compounds

278    5 and 6, indicating that the hydroxylation of benzene ring in DPA structure is not a

279    dominating process by direct photolysis under UVC irradiation. It should be noted that the

280    different chemical shifts of compounds 5 and 6 in both spectra (B) and (C) resulted from the

281    effect of different final pH, such as pH 6.47 in the direct photolysis but pH 5.56 in the

282 photocatalysis. Water samples were extracted with chloroform to concentrate the organics for

283 further analysis. As a result, it was identified that some multi-hydroxylated products

284 (compounds 8–12, $n_{OH}$ = 2–5) appeared in the TiO$_2$/UVA process but not in the UVC process

285 when corroborating with their mass ion peaks in LC-MS spectra. NMR spectra of organic

286 extracts are not presented in this paper.

287

288 *3.4. Degradation pathways*

289    The results in Table 2 reflect a fact that there are different pathways between the DPA

290 degradations in photolytic and photocatalytic processes due to the evolution of different

291 principal intermediates. Figure 3 illustrates the proposed pathways of DPA degradation by

292 UVC irradiation alone, which may not include every possible reactions but covering the main

293 approaches confirmed by the identified products. The major decay pathways include N-

294 methyl oxidation, scission of the N-CO or C-CO bond, dimerization and ring opening. The

295 results have been compared to those from previous research with analogous degradation

296 mechanisms such as tyrosine, phenylthioacetic acid and phenylurea derivatives photolysis

297 (Jin et al., 1995; Filipiak et al., 2006), which are similar to our findings. For specific

298 intermediates, compound 1, arising from N-methyl oxidation, is considered to be the major

299 primary intermediate in the process (see Fig. 2). The oxidation of terminal methyl group

300 involves an intramolecular hydrogen bond between N-methyl and carbonyl groups in the

301 excited state (Jirkovský et al., 1997), and then reacts with dissolved molecular oxygen to

302 form formylated product [–N(CH$_3$)CHO]. This indicates a key role played by the

303 photoexcited oxygen species and the formation of the formylated product by oxidation of the

304 *N*-methyl group was the major reaction observed. The subsequent reduction and further

305 oxidation of compound 1 gave rise to form compounds 2 and 3, in which compound 3 easily

306 underwent the decarboxylation to yield compound 4 via photo-kolbe reactions (Krautler and

307  Bard, 1978). The evolution profiles of compounds 1–4 in Fig. 2 offer useful information in

308  supporting this pathway. On the other hand, no products that obviously come from further

309  oxidation of the second N-methyl group were detected in our experiments. Despite

310  hydroxylated products 5 and 6 were detected, the fact that they only existed at trace levels

311  and implied that hydroxylation of aromatic ring was not a minor pathway in the UVC

312  photolysis process.

313  [Fig. 3]

314

315       Direct irradiation leads to the promotion of a molecule from the ground state to an excited

316  state. Such excited states can undergo homolysis or heterolysis, among other processes. It is

317  known that a 254 nm photon has an equivalence of 4.89 eV, which should be enough

318  energetic to produce homolytic or heterolytic breakages in the molecules (Litter, 2005).

319  Therefore, it can be expected that further photolysis bond scission could take place, followed

320  by radical recommendation or H-/(HO-) abstracting from water solvent. For instance, scission

321  of the N-CO bond leads to yield the diphenylacetic acid (compound 15) while scission of the

322  C-CO bond gives benzhydrol (compound 16) as a major intermediate and a trace amount of

323  compound 13. The cleavage of compound 16 can produce small molecules such as phenol

324  (compound 17) and benzaldehyde (compound 18), where benzaldehyde can easily undergo

325  further oxidation to form secondary intermediate benzoic acid (compound 19) while phenol

326  trends to undergoing the ring opening to form product 20. The observed product 20,

327  belonging to an aliphatic polyene acid, can be successively transformed into product 21 and

328  finally to $CO_2$ and $H_2O$. A similar pathway for phenol degradation by photolysis was

329  proposed by Jin et al. (1995).

330       In the heterogeneous photocatalysis process with $TiO_2$/UVA, hydroxylation reactions of

331  the aromatic ring are the most frequently observed primary reaction due to the attack of •OH

332 (Amine-Khodja et al., 2002). Similarly, these reactions were proposed in Fig. 4, which are

333 significantly different from that of DPA photolytic process. First, isomers 5-7 were identified

334 as the phenolic compounds monosubstituted by OH in para-, ortho- and meta-position,

335 respectively, suggesting that the aromatic ring has an electron-donating effect, due to the

336 electrophilicity of hydroxyl radicals. It is interesting that isomer 5 shows the highest

337 concentration level, following by isomers 6 and 7. These results indicate that the

338 monohydroxylation of aromatic ring with corresponding H abstraction by •OH attack not

339 only is a major reaction step in the photocatalytic process but also takes place regioselectively

340 on the aromatic ring. By further attack of •OH, its subsequent reaction with oxidizing species

341 yielded the multihydroxylated intermediates (compounds 8–12), such as di-, tri-, tetra- and

342 quint-substitution phenolics. However, the low concentrations of these products reveal that

343 the multihydroxylation reaction might occur just as a minor route in the photocatalytic

344 degradation of DPA. Further oxidation by •OH attack can result in the benzene ring opening

345 to yield maleic acid (compound 21). The ring opening is possibly due to the formation of a

346 hydroxycyclohexadienyl radical in photocatalysis process (e.g. radical B in Fig. 4), confirmed

347 by Aceituno et al. (2002). Besides this, both oxidation of N-methyl groups and N-

348 demethylation on the urea moiety of DPA were also proposed, as shown in Fig. 5. These

349 reactions were conducted through attack by hydroxyl radicals and reaction with oxygen.

350 Although the compounds 1-4 were found in both photolysis and photocatalysis, their

351 evolution underwent different reactions by bond scission and •OH attack, respectively.

352 [Fig. 4]

353 [Fig. 5]

354

355 **4. Conclusions**

356     The experiments demonstrated that DPA degradation by direct photolysis with UVC

357 proceeded quickly, but its further mineralization was difficult, while the DPA degradation by

358 photocatalysis with TiO$_2$/UVA proceeded more slowly, but achieved a higher extent of

359 mineralization. Using both the LC–MS and ^{1}H–NMR analyses together is a powerful

360 approach to identify more than 20 intermediates from the DPA degradation. The analytical

361 results indicate that two processes undergo some similar reactions such as the oxidation of N-

362 methyl group of side chain, but also undergo some different approaches. For example, the

363 hydroxylation of aromatic ring was observed as a major way in the photocatalytic process

364 while it is a minor one in the direct photolytic process. This fundamental research about the

365 mechanism of photolytic and photocatalytic reaction provides essential knowledge with

366 potential to further develop a best process for aqueous DPA degradation in water treatment.

367

371 **Supplemental Material**
372
373 Supplementary data associated with this article can be found, in the online version, at xxxxxx.
374

375 **References**

376 Aceituno, M., Stalikas, C.D., Lunar, L., Rubio, S., Pérez-Bendito, D., 2002. H$_2$O$_2$/TiO$_2$

377     photocatalytic oxidation of metol: identification of intermediates and reaction pathways.

378     Water Res. 36, 3582–3592.

379 Amine-Khodja, A., Lavédrine, B., Richard, C., Sehili, T., 2002. Photocatalytic degradation of

380     metoxuron in aqueous suspensions of TiO$_2$: analytical and kinetic studies. Int. J.

381     Photoenergy 4, 147–151.

382   Es-Safi, N.E., Guernevé, C.L., Cheynier, V., Moutounet, M., 2000. New phenolic

383       compounds obtained by evolution of (+)-catechin and glyoxylic acid in hydroalcoholic

384       medium. Tetrahedron Lett. 41, 1917–1921.

385   Filipiak, P., Hug, G.L., Marciniak, B., 2006. Photochemistry of carboxylic acids containing

386       the phenyl and thioether groups: steady-state and laser flash photolysis studies. J.

387       Photochem. Photobiol. A 177, 295–306.

388   Jin, F., Leitich, J., Sonntag, C.V., 1995. The photolysis ($\lambda$ = 254 nm) of tyrosine in aqueous

389       solutions in the absence and presence of oxygen: the reaction of tyrosine with singlet

390       oxygen. J. Photochem. Photobiol. A 92, 147-153.

391   Jirkovský, J., Faure, V., Boule, P., 1997. Photolysis of diuron. Pestic. Sci. 50, 42-52.

392   Krautler, B., Bard, A.J., 1978. Heterogeneous photocatalytic synthesis of methane from

393       acetic acid - new Kolbe reaction pathway. J. Am. Chem. Soc. 100, 2239-2240.

394   Liang, H.C., Li, X.Z., 2009. Effects of structure of anodic $TiO_2$ nanotube arrays on

395       photocatalytic activity for the degradation of 2,3-dichlorophenol in aqueous solution. J.

396       Hazard. Mater. 162, 1415-1422.

397   Limiroli, R., Consonni, R., Ranalli, A., Bianchi, G., Zetta, L., 1996. ^{1}H NMR study of

398       phenolics in the vegetation water of three cultivars of *olea europaea*: similarities and

399       differences. J. Agr. Food Chem. 44, 2040-2048.

400   Litter, M.I., 2005. Introduction to photochemical advanced oxidation processes for water

401       treatment. The Handbook of Environmental Chemistry, Vol. 2, Part M, Environmental

402       Photochemistry Part II. Springer-Verlag, Berlin.

403   Pavia, D.L., Lampman, G.M., Kriz, G.S., 2001. Introduction to Spectroscopy: A Guide for

404       Students of Organic Chemistry 3rd ed., Brooks/Cole, , Singapore, pp. 266-267.

405    Rahman, M.A., Muneer, M., Bahnemann, D., 2003. Photocatalysed degradation of a

406        herbicide derivatives, diphenamid in aqueous suspension of titanium dioxide. J. Adv.

407        Oxid. Technol. 6, 100–108.

408    Rosen, J.D., 1967. The photolysis of diphenamid. B. Environ. Contam. Tox. 2, 349-354.

409    Schultz, D.P., Tweedy, B.G., 1972. The effect of light and humidity on absorption and

410        degradation of diphenamid in tomatoes. J. Agr. Food Chem. 20, 10-13.

411    Sirons, G.J., Zilkey, B.F., Frank, R., Paik, N.J., 1981. Residues of diphenamid and its

412        phytotoxic metabolite in flue-cured tobacco. J. Agr. Food Chem. 29, 661-664.

413    Sleiman, M., Ferronato, C., Fenet, B., Baudot, R., Jaber, F., Chovelon, J.M., 2006.

414    Development of HPLC/ESI-MS and HPLC/1H NMR methods for the identification of

415    photocatalytic degradation products of iodosulfuron. Anal. Chem. 78, 2957-2966.

417

418

419 **List of figure captions**

420 Fig. 1. The full-scan mass spectra in the m/z 50-400 range for the degradation of DPA by

421      photolysis (a) and $TiO_2$-photocatalysis (b).

422 Fig. 2. ^{1}H-NMR analysis of DPA degradation by UVC and $TiO_2$/UVA treatments: (a) 2D-

423      COSY spectra of aqueous DPA solutions, in which the proton signals of methine group

424      in DPA and compounds 1–4 were marked; (b) Relevant region of 1D ^{1}H-NMR spectra

425      of DPA and its hydroxylation products 5, 6 and 7.

426 Fig. 3. Proposed pathways of the DPA degradation by direct photolysis with UVC.

427 Fig. 4. Proposed pathways of the DPA degradation by photocatalysis with $TiO_2$/UVA. Here,

428      R1 is p- or m-phenolic ring; R2 is 3,5-diphenolic ring; and R' includes benzene ring, R1,

429      and R2.

430 Fig. 5. Mechanism of oxidation of N-methyl group in DPA molecules by photocatalysis

432

433    Table 1. Effects of solution pH on DPA degradation efficiency, kinetic constants, correlation

434    coefficients and DOC removal by different systems after 360 min reaction. Here, $C_0$ =

435    20 mg L$^{-1}$.

| System | DPA decay (1–C/C$_o$, %) | | | $k^a \times 10^{-3}$ (min$^{-1}$)/R$^2$ | | | DOC removal (%) | | |
|---|---|---|---|---|---|---|---|---|---|
| | pH 3.5 | 7.2 | 9.6 | pH 3.5 | 7.2 | 9.6 | pH 3.5 | 7.2 | 9.6 |
| UVC | 100 | 100 | 100 | 32/0.999 | 19/0.979 | 24/0.998 | 11 | 8 | 9 |
| UVA | –[b] | – | – | – | – | – | – | – | – |
| TiO$_2$/UVA | 63 | 51 | 42 | 1.8/0.979 | 1.3/0.994 | 1.0/0.978 | 13 | 11 | 8 |

436    [a] - The pseudo-first order kinetic constant
437    [b] - not detected.
438

439

440

441

442

443

444

445

446

447
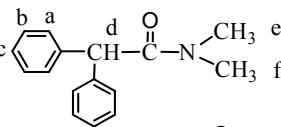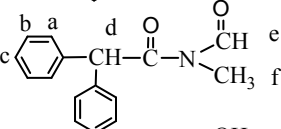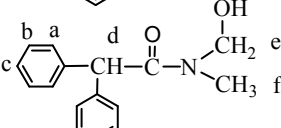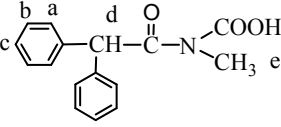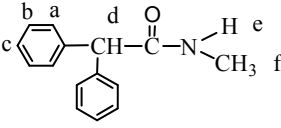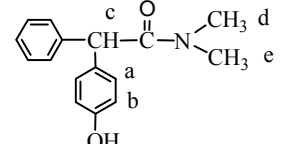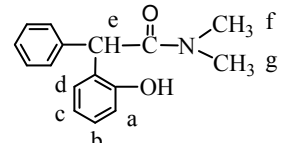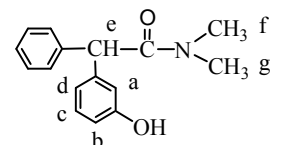
448

449

450

Table 2. Products resulting from the direct photolysed and photocatalysed degradation of DPA by MS and ^{1}H-NMR analysis.

Other products 8-21 were shown in Table SM-1.

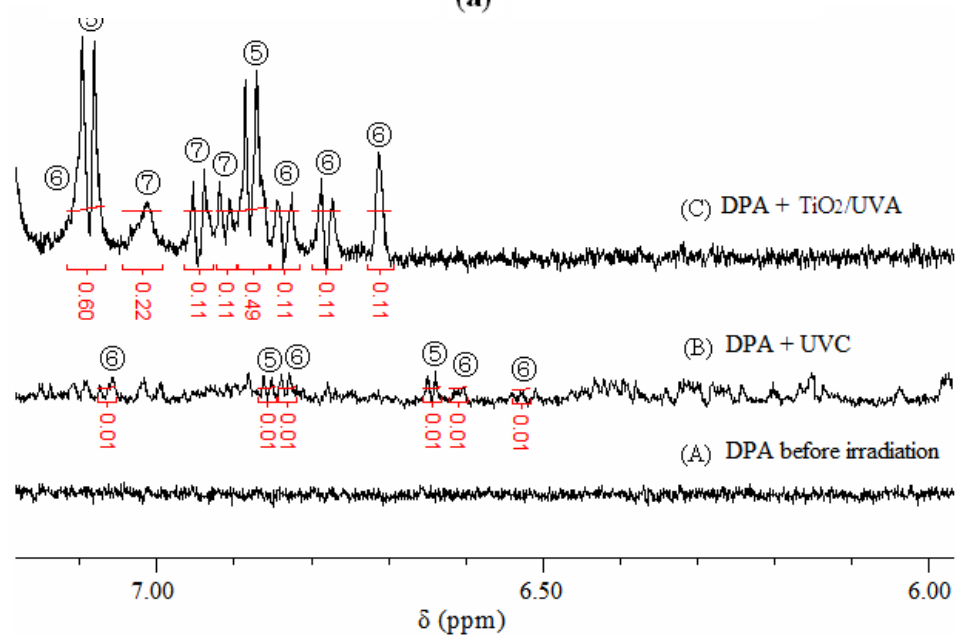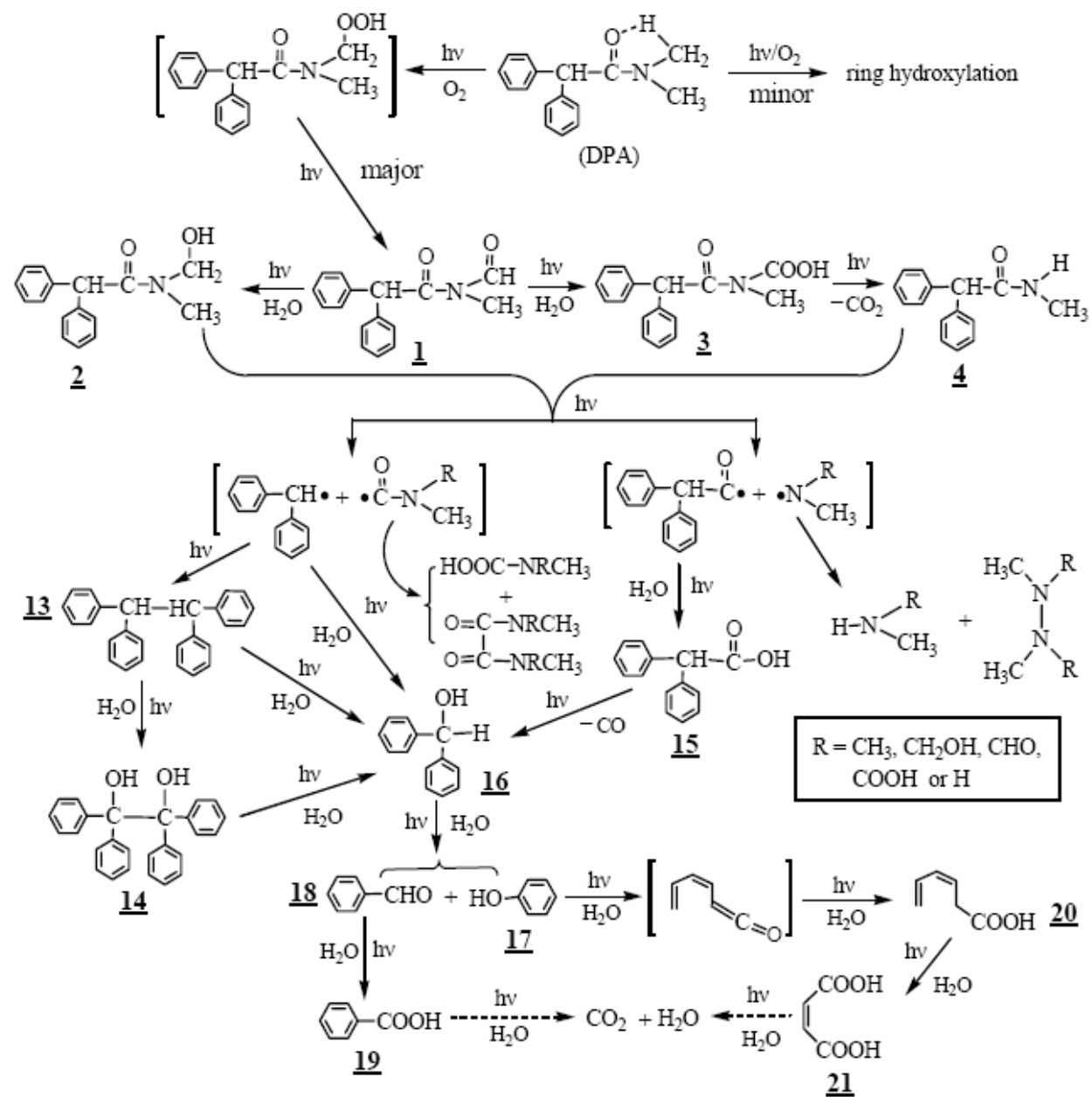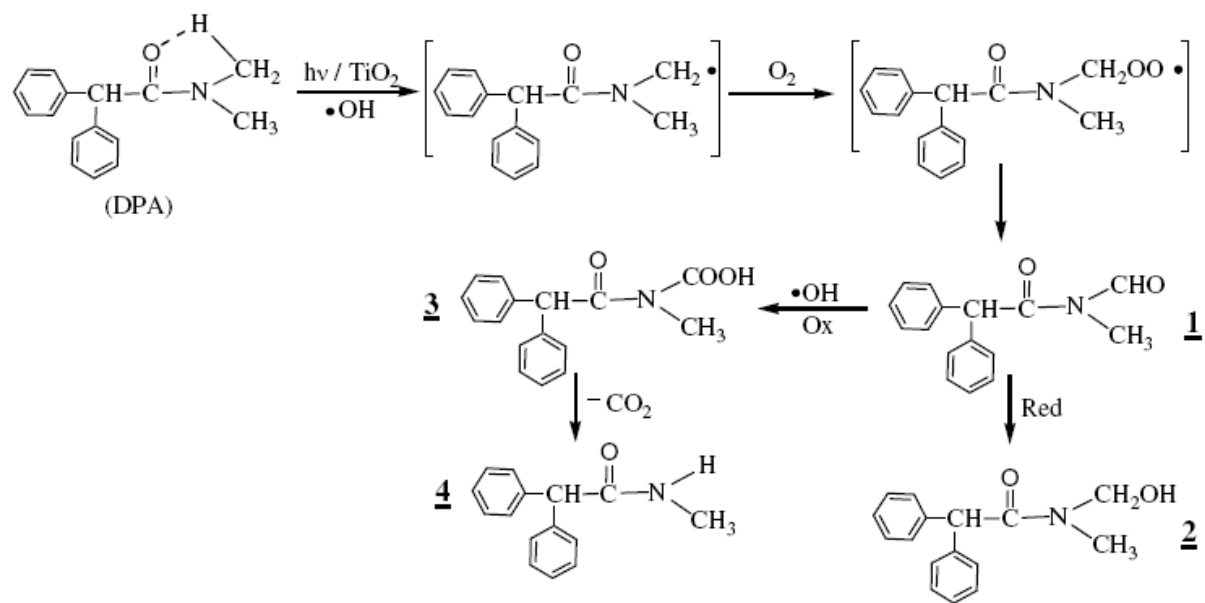| Compound No. | Structures[a] | MS data (m/z) | ^{1}H-NMR data (δ, multiplicity[b], coupling constant) | Products of DPA degradation[c] UVC | Products of DPA degradation[c] TiO$_2$/UVA |
|---|---|---|---|---|---|
| DPA | (structure) | 238 (M-H)$^-$ 240 (M+H)$^+$ 241 (M+2H)$^{++}$ | a: 7.22 (4H, d, $J_{ab}$ = 8.56); b: 7.41 (4H, m); c: 7.35 (2H, t, $J_{cb}$ = 7.18); d: 5.58 (1H, s); e: 3.04 (3H, s); f: 3.00 (3H, s) | + | + |
| 1 | (structure) | 251 (M+O-2H)$^{--}$ 254 (M+O+H)$^+$ 255 (M+O+2H)$^{++}$ | a: 7.22 (4H, d, $J_{ab}$ = 8.56); b: 7.41 (4H, m); c: 7.35 (2H, t, $J_{cb}$ = 7.18); d: 5.52 (1H, s); e: 8.44 (1H, s); f: 3.11 (3H, s) | + | + |
| 2 | (structure) | 255 (M+O) 256 (M+O+H)$^+$ 258 (M+O+3H)$^{+++}$ | a: 7.22 (4H, d, $J_{ab}$ = 8.56); b: 7.41 (4H, m); c: 7.35 (2H, t, $J_{cb}$ = 7.18); d: 5.64 (1H, s); e: 5.89 (2H, s); f: 3.04 (3H, s) | + | + |
| 3 | (structure) | 268 (M+2O-H)$^-$ 270 (M+2O+H)$^+$ 271 (M+2O+2H)$^{++}$ | a: 7.22 (4H, d, $J_{ab}$ = 8.56); b: 7.41 (4H, m); c: 7.35 (2H, t, $J_{cb}$ = 7.18); d: 5.49 (1H, s); e: 3.08 (3H, s) | + | + |
| 4 | (structure) | 224 (M-CH$_2$-H)$^-$ 226 (M-CH$_2$+H)$^+$ 227 (M-CH$_2$+2H)$^{++}$ | a: 7.22 (4H, d, $J_{ab}$ = 8.56); b: 7.41 (4H, m); c: 7.35 (2H, t, $J_{cb}$ = 7.18); d: 5.43 (1H, s); e: 7.51 (H, m); f: 2.99 (3H, d, $J_{fe}$ = 4.05) | + | + |
| 5 | (structure) | 254 (M+O-H)$^-$ 256 (M+O+H)$^+$ 257 (M+O+2H)$^{++}$ | a: 7.10 (2H, d, $J_{ab}$ = 9.11); b: 6.88 (2H, d, $J_{ba}$ = 9.09); c: 5.58 (1H, s); d: 3.04 (3H, s); e: 3.00 (3H, s) | trace | + |
| 6 | (structure) | 254 (M+O-H)$^-$ 256 (M+O+H)$^+$ 257 (M+O+2H)$^{++}$ | a: 6.91 (1H, d, $J_{ab}$ = 8.79); b: 7.01 (1H, m); c: 7.01 (1H, m); d: 6.95 (1H, d, $J_{dc}$ = 8.58); e: 5.58 (1H, s); f: 3.04 (3H, s); g: 3.00 (3H, s) | trace | + |
| 7 | (structure) | 254 (M+O-H)$^-$ 256 (M+O+H)$^+$ 257 (M+O+2H)$^{++}$ | a: 6.71 (1H, s); b: 6.78 (1H, d, $J_{bc}$ = 9.75); c: 7.09 (1H, m); d: 6.84 (1H, d, $J_{dc}$ = 9.50); e: 5.58 (1H, s); f: 3.04 (3H, s); g: 3.00 (3H, s) | trace | + |

[Fig. 1]



(a)

(b)

[Fig. 2]



(a)

(b)

[Fig. 3]

[Fig. 4]
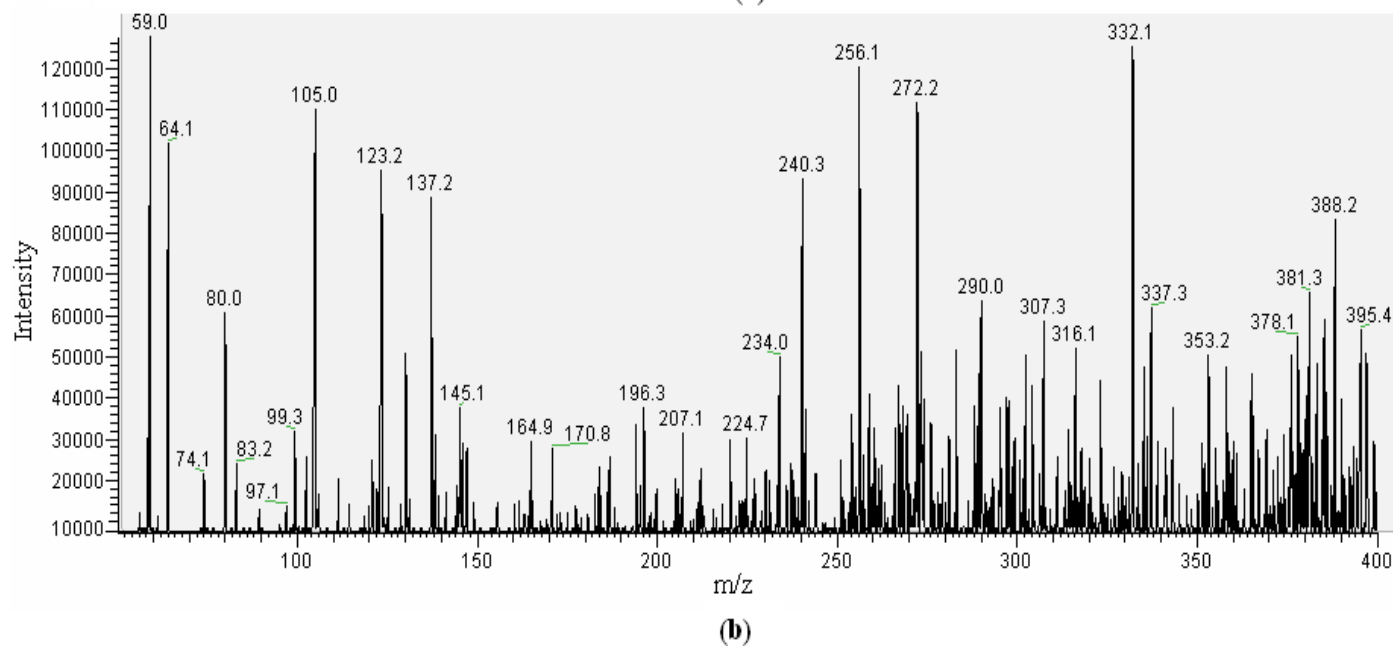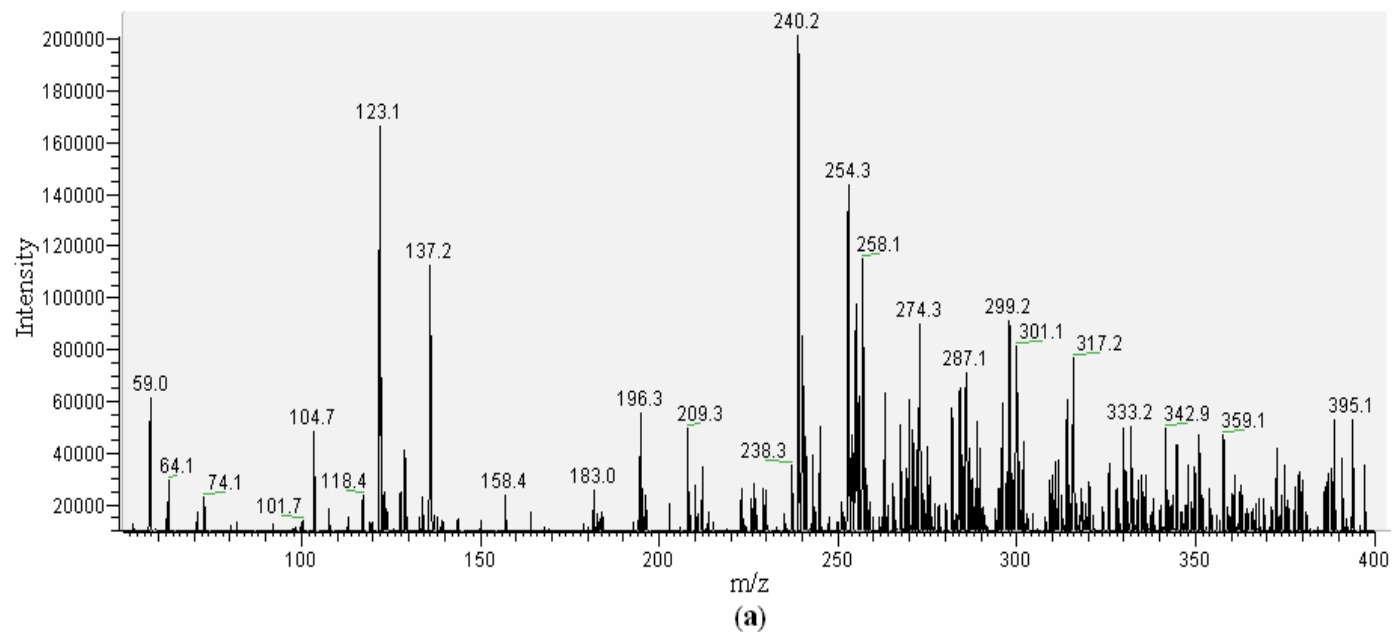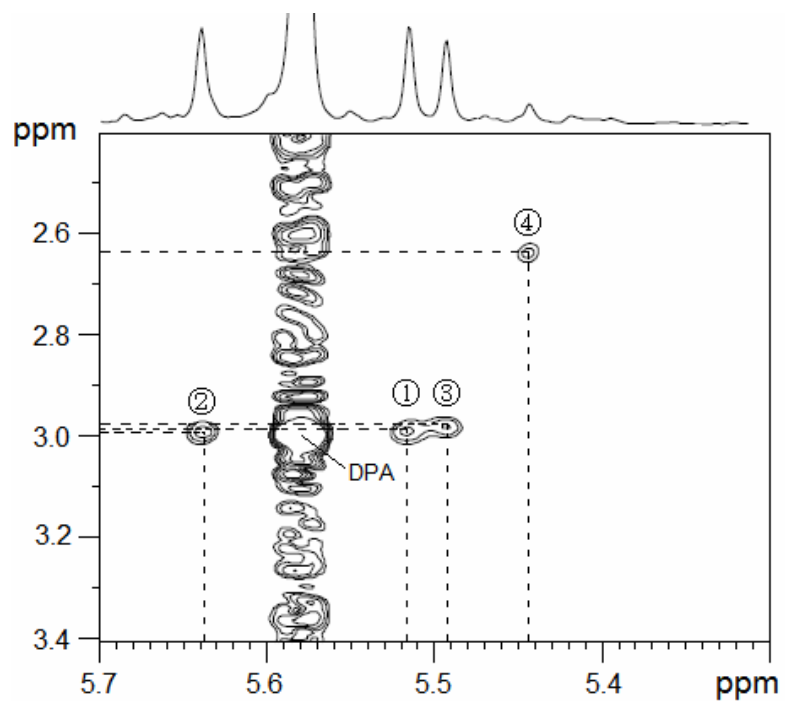
[Fig. 5]

Supplemental Material:

[Fig. SM-1]  Diagram of the batch-scale photocatalytic-reactor.



Photocatalytic-reactor
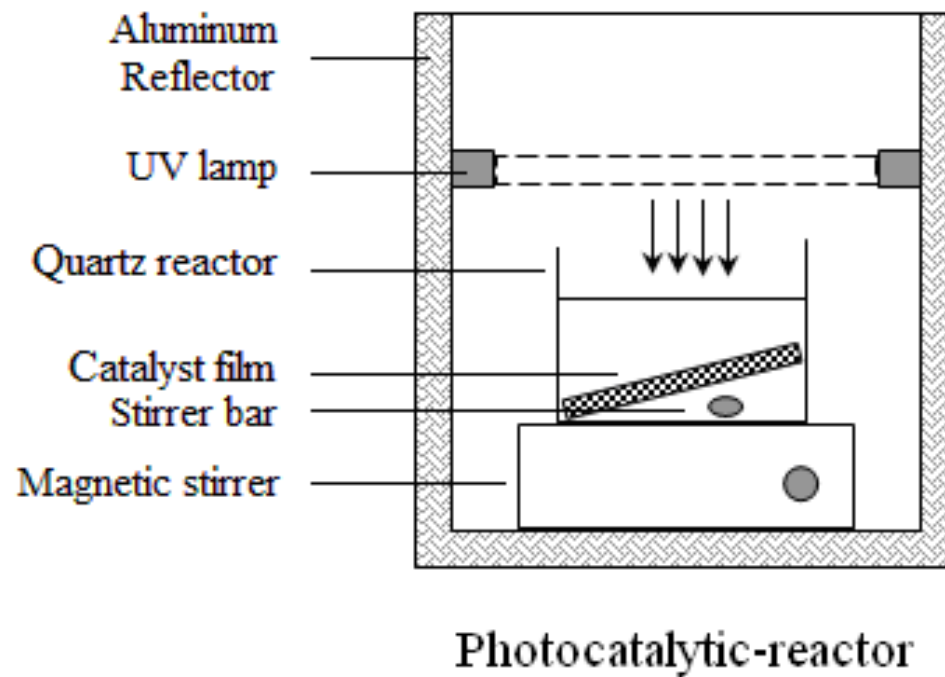
[Fig. SM-2]   UV-visible spectra of aqueous DPA solutions at different pH media before irradiation.
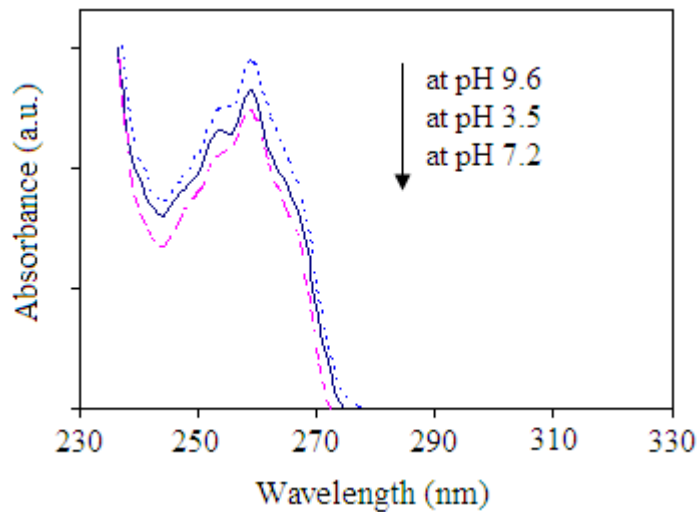


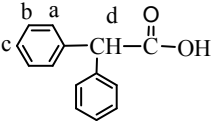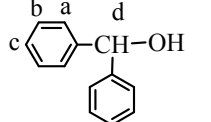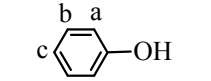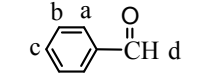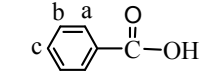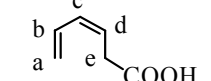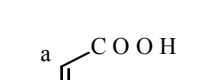(The color figure is intended to be reproduced in black-and-white.)

Table SM-1. Products 8-12 resulting from the direct photolysed and TiO$_2$-photocatalysed degradation of DPA by MS and $^1$H-NMR analysis.

| Compound No. | Structures[a] | MS data (m/z) | $^1$H-NMR data (δ, multiplicity[b], coupling constant) | Products of DPA degradation[c] UVC | Products of DPA degradation[c] TiO$_2$/UVA |
|---|---|---|---|---|---|
| 8[d] |  | 272 (M+H)$^+$ <br> 273 (M+2H)$^{++}$ <br> 274 (M+3H)$^{+++}$ | a: 6.63 (2H, s); b: 6.57 (1H, s); <br> c: 5.58 (1H, s); d: 3.04 (3H, s); <br> e: 3.00 (3H, s) | – | trace |
| 9[d] |  | 272 (M+H)$^+$ <br> 273 (M+2H)$^{++}$ <br> 274 (M+3H)$^{+++}$ | a: 5.58 (1H, s); b: 3.04 (3H, s); <br> c: 3.00 (3H, s) | – | trace |
| 10[d] |  | 285 (M-3H)$^{---}$ <br> 288 (M+H)$^+$ <br> 290 (M+3H)$^{+++}$ | a: 6.63 (2H, s); b: 6.57 (1H, s); <br> c: 5.58 (1H, s); d: 3.04 (3H, s); <br> e: 3.00 (3H, s) | – | trace |
| 11[d] |  | 300 (M-3H)$^{---}$ <br> 303 (M) <br> 304 (M+H)$^+$ <br> 306 (M+3H)$^{+++}$ | a: 6.63 (2H, s); b: 6.57 (1H, s); <br> c: 5.58 (1H, s); d: 3.04 (3H, s); <br> e: 3.00 (3H, s) | – | trace |
| 12[d] |  | 316 (M-3H)$^{--}$ <br> 318 (M-H)$^-$ <br> 322 (M+3H)$^{+++}$ <br> 323 (M+4H)$^{++++}$ | a: 6.63 (2H, s); b: 6.57 (1H, s); <br> c: 5.58 (1H, s); d: 3.04 (3H, s); | – | trace |
| 13[d] |  | 332 (M-2H)$^{--}$ <br> 333 (M-H)$^-$ <br> 336 (M+2H)$^{++}$ | a: 7. 51(4H, d, $J_{ab}$ = 8.22); b: 7.53 (4H, m); <br> c: 7.45 (2H, t, $J_{cb}$ = 8.14); d: 4.89 (1H, s); | + | – |
| 14[d] |  | 365 (M-H) <br> 366 (M) <br> 367 (M+H)$^+$ | a: 7. 49 (5H,s) | + | – |

Table SM-1 (Continue)

| Compound No. | Structures[a] | MS data (m/z) | $^1$H-NMR data ($\delta$, multiplicity[b], coupling constant) | Products of DPA degradation[c] | |
|---|---|---|---|---|---|
| | | | | UVC | TiO$_2$/UVA |
| **15** |  | 211 (M-H)$^-$ 212 (M) 213 (M+H)$^+$ | a: 7. 22 (4H, d, $J_{ab}$ = 8.56); b: 7.41 (4H, m); c: 7.35 (2H, t, $J_{cb}$ = 7.18); d: 5.12 (1H, s); | + | + |
| **16** |  | 183 (M-H)$^-$ 184 (M) 185 (M+H)$^+$ | a: 7.39 (4H, d, $J_{ab}$ = 8.02); b: 7.51 (4H, m); c: 7.47 (2H, t, $J_{cb}$ = 8.81); d: 5.89 (1H, s); | + | + |
| **17**[d] |  | 93 (M-H)$^-$ 94 (M) 95 (M+H)$^+$ | a: 6.85 (2H, d, $J_{ab}$ = 6.54); b: 7.25 (2H, m); c: 6.99 (1H, t, $J_{cb}$ = 7.55) | trace | trace |
| **18** |  | 105 (M-H)$^-$ | a: 7.89 (2H, d, $J_{ab}$ = 9.24); b: 7.51 (2H, m); c: 7.74 (1H, t, $J_{cb}$ = 8.31); d: 9.34 (1H, s); | + | + |
| **19** |  | 121 (M-H)$^-$ 122 (M) 123 (M+H)$^+$ | a: 8.16 (2H, d, $J_{ab}$ = 9.20); b: 7.67 (2H, m); c: 7.49 (1H, t, $J_{cb}$ = 8.12); | + | + |
| **20**[d] |  | 111 (M-H)$^-$ 112 (M) 113 (M+2H)$^{++}$ | a: 5.83 (2H, d, $J_{ab}$ = 8.91); b: 6.15 (1H, m); c: 6.44 (1H, m); d: 5.97 (1H, m); e: 3.38 (2H, d, $J_{ed}$ = 3.85); | + | − |
| **21**[d] |  | 115 (M-H)$^-$ 118 (M+2H)$^{++}$ | a: 6.36 (2H, s) | − | + |

[a] Different protons linked on molecular structures are marked as a, b, c, d, e and f, respectively.
[b] Singlet, doublet, triplet, and multilet are abbreviated as s, d, t and m, respectively; coupling constants ($J$) are given hertz.
[c] −, absence; +, presence.
[d] Identified in organic extracts only. The NMR spectra of organic extracts were not showed in the present paper.